

## Temperature and localization of atoms in three-dimensional optical lattices

M. Gatzke, G. Birkl,\* P. S. Jessen,† A. Kastberg,‡ S. L. Rolston, and W. D. Phillips  
 PHYS A167, National Institute of Standards and Technology, Gaithersburg, Maryland 20899

(Received 10 January 1997)

We report temperature measurements of atoms trapped in a three-dimensional (3D) optical lattice, a well-defined laser-cooling situation that can be treated with currently available theoretical tools. We also obtain fluorescence spectra from a 3D optical lattice, from which we obtain quantitative information about the trapping atoms, including the oscillation frequencies, spatial localization, and a temperature, which is in good agreement with our direct measurements. For comparison we study a 1D lattice using the same atom (cesium).  
 [S1050-2947(97)50506-3]

PACS number(s): 32.80.Pj, 42.50.Vk

Given the emergence of laser cooling of neutral atoms as a standard laboratory technique now used in a host of applications, it is surprising that few direct comparisons of theory and experiment have been made concerning the equilibrium atomic momentum distribution (or temperature) achieved by laser cooling. While a recent experiment in one-dimension (1D) [1] agreed quantitatively with a theoretical simulation [2], comparisons in 3D are lacking, primarily for two reasons: the difficulty of extending calculations to 3D [3,4] and the lack of appropriate experiments. To date, the only measurements of temperature in 3D laser-cooled samples were obtained in magneto-optical traps (MOTs) [5] or optical molasses, each created with six laser beams where the phases between the beams were not controlled [6,7]. Under these circumstances the morphology of the optical potential (due to the ac Stark shift) varies in time, which is a difficult situation to model. More amenable to theoretical treatment are time-invariant optical potentials called “optical lattices,” which are a version of optical molasses having a spatially periodic arrangement of sites of pure circular polarization. With the lasers tuned below atomic resonance the atoms are cooled, and optical dipole forces trap the atoms at these sites. While such systems have already been studied in 1D [1,8], 2D [9,10], and 3D [10–14], we report here the measurements of temperature in any optical lattice beyond 1D. We also present fluorescence spectra from a 3D optical lattice, with sufficient resolution to observe motional sidebands. The spectra reveal both the spatial localization and temperature of the atoms in addition to other dynamical information, including oscillation frequencies and motional relaxation. All our observations are self-consistently interpreted using an analytic, anharmonic oscillator model.

We create a 3D optical lattice with four laser beams [15]: two orthogonally polarized pairs of beams that propagate in planes perpendicular to each other with a 90° angle between the beams of each pair, ( $\hat{\epsilon}_y(\pm\hat{x}-\hat{z}), \hat{\epsilon}_x(\pm\hat{y}+\hat{z})$ ), as in [14]. This is a simple extension [11] of the 1D linLin

optical molasses [a pair of orthogonally polarized, counter-propagating beams ( $\hat{\epsilon}_y(-\hat{x}), \hat{\epsilon}_z(+\hat{x})$ )], which we also studied for comparison. In the 1D case, the interference of the beams creates a set of planes of pure circular polarization ( $\sigma^+$  and  $\sigma^-$  alternately) spaced by  $\lambda/4$ , where  $\lambda$  is the wavelength of the lattice light. In 3D there are sites of pure  $\sigma^+$  and  $\sigma^-$  polarization [with respect to the symmetry axis ( $z$ )] alternately arranged on a centered tetragonal lattice with lattice constants of  $a_{x,y}=\lambda/\sqrt{2}$  and  $a_z=\lambda/2\sqrt{2}$ . We load the lattice with Cs atoms captured in a MOT and then laser cooled for 1 ms in a six-beam  $\sigma^+-\sigma^-$  optical molasses [14]. We turn off the molasses, leaving the atoms in an optical lattice tuned 5–15 natural line widths ( $\Gamma/2\pi=5.22$  MHz) red of the  $D2$  resonance at 852 nm ( $F=4\rightarrow F'=5$ ). The sequence (MOT→molasses→lattice) is typically cycled at a frequency of 125 Hz with a 4-ms lattice phase.

Using a time-of-flight (TOF) technique, after a sudden release of atoms from the lattice [14], we measure a Gaussian distribution of momentum  $p_x$  along the vertical ( $x$ ) direction and determine the temperature,  $k_B T = \langle p_x^2 \rangle / m$ . We measure  $T$  (found to be isotropic within the 30% uncertainties in [14]) as a function of laser intensity for three different detunings  $\Delta$  from atomic resonance. Figure 1 (full circles) shows typical results for a 3D data run at  $\Delta = -5.2\Gamma$  as a function of light shift potential  $U_0$  [16]. The two-level approximation for the potential, including saturation and for  $\Delta \gg \Gamma$ , can be written as  $U_0 = \hbar(|\Delta|/2) \ln[1 + (44/45)\Omega_{\text{Rabi}}^2/2\Delta^2]$ . Here,  $\Omega_{\text{Rabi}}^2 = (\Gamma^2/2)(I/I_0)$  is the square of the maximum Rabi frequency (at the center of a potential well),  $I$  is the maximum light intensity there ( $I = 8I_{\text{beam}}$ , where  $I_{\text{beam}}$  is the intensity of a single beam), and  $I_0 = 1.1$  mW/cm<sup>2</sup>. Since the atoms are predominantly localized in sites of pure circular polarization and optically pumped to the extreme  $m$  states, this analytic two-level approximation is appropriate. From the figure it is clear that  $T$  scales linearly with  $U_0$ . From analysis of all data runs we find a mean value for the slope of  $C_{3D} = k_B(T - T_0)/2U_0 = 0.121(14)$ , independent of the detuning within the uncertainty of our measurements. The uncertainty ( $1\sigma$ ) includes both the run-to-run scatter in the measured slopes and calibration of the laser intensity. We attribute the run-to-run scatter to irreproducibility in our measurements of intensity and detuning. In Fig. 1 we plot similar results obtained for the 1D lattice (along the vertical

\*Present address: Institut für Quantenoptik, Universität Hannover, Welfengarten 1, D-30167, Hannover, Germany.

†Present address: University of Arizona, Tucson, AZ 85721.

‡Present address: Stockholm University, Frescativägen 24, S-104 05 Stockholm, Sweden.

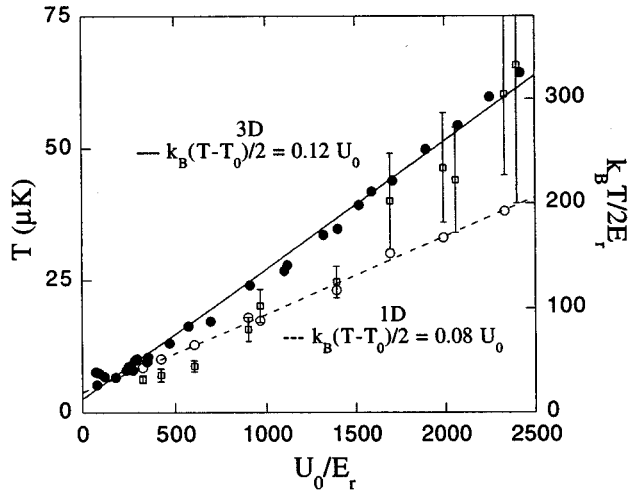


FIG. 1. Temperature in the 3D (●) and 1D (○) lattices measured by time of flight vs the maximum light shift  $U_0$  scaled by the recoil energy  $E_r$ , for a lattice detuning of  $\Delta = -5.2\Gamma$ ,  $-5.7\Gamma$ , respectively, along with best fits. Also shown are 1D temperatures (□) obtained from the fluorescence spectrum at  $\Delta = -5.7\Gamma$ .

direction) for  $\Delta = -5.7\Gamma$ . Again we observe a linear scaling of  $T$  with  $U_0$ , but the proportionality constant,  $C_{1D} = 0.079(10)$ , is smaller than in 3D. These measurements of  $C$  are similar to the one reported previously in 1D [1], to the predictions of 1D calculations [2,3], and to measurements of  $C$  in a phase-uncontrolled 3D optical *molasses* [6,7] if the average intensity ( $I = 6I_{\text{beam}}$ ) is used to determine  $U_0$ .

Our temperature measurements confirm that polarization-gradient (or Sisyphus) laser cooling in the 3D lattice produces temperatures so low that an atom is trapped in a single well, i.e.,  $k_B T \ll U_0$ . From the known shape of the potential and the virial theorem, we use our measurements of  $T$  to infer the equilibrium spatial distribution (or localization) along  $x$  (vertical) within each well. In addition, we can mea-

sure the localization (in any direction) through a high-resolution spectral analysis of the light that is scattered by the atoms in the lattice. Below we will compare the results of this direct measurement, described next, with the localization inferred from our temperature measurements.

In a harmonic approximation, valid near the bottom of the wells, the 3D potential is separable:  $U(x, y, z) = U_0(K_x^2 x^2 + K_y^2 y^2 + K_z^2 z^2)$ . The virial theorem ( $\langle U(x, y, z) \rangle = 3k_B T/2$ ) implies  $\langle K_\xi^2 \xi^2 \rangle = C$ , ( $\xi \in \{x, y, z\}$ ). Since  $C \ll 1$ , the atoms are spatially localized within the wells, and since  $K \approx k = 2\pi/\lambda$  we are in the Lamb-Dicke regime [17] ( $\xi_{\text{rms}} \leq \lambda/2\pi$ ), where perfectly elastic (recoilless) scattering of the light predominates over inelastic scattering in which the atoms recoil. In this regime the ratio of inelastic to elastic scattering  $\mathfrak{R}$  yields the localization  $k\xi_{\text{rms}}$  along the observation direction:  $\mathfrak{R} = (k\xi_{\text{rms}})^2$  [18]. In addition, the inelastic part of the spectrum reveals information about the motion of atoms, including the oscillation frequencies in the wells and the temperature [1], discussed below. Some of this same dynamical information is available from probe absorption spectroscopy [8–11] or from four-wave mixing spectroscopy [12], but these techniques do not directly yield information about either the temperature or localization of atoms in the lattice.

To obtain an ultrahigh resolution power spectrum of the scattered light, we use an optical heterodyne technique [1,19], where we combine the scattered light with a frequency-shifted (by  $\approx 50$  MHz) local oscillator beam on a photodiode. The rf beat signal from the diode is mixed down, sampled and fast-Fourier transform (FFT) analyzed with 256 points. After background subtraction and signal averaging we obtain spectra like those shown in Fig. 2, each of which was obtained in  $\sim 30$  minutes. Our spectrum is similar to the Fourier transform of the autocorrelation of fluorescence obtained in a related experiment [20], although in that case only positive frequencies are measured and no temperature information is available.

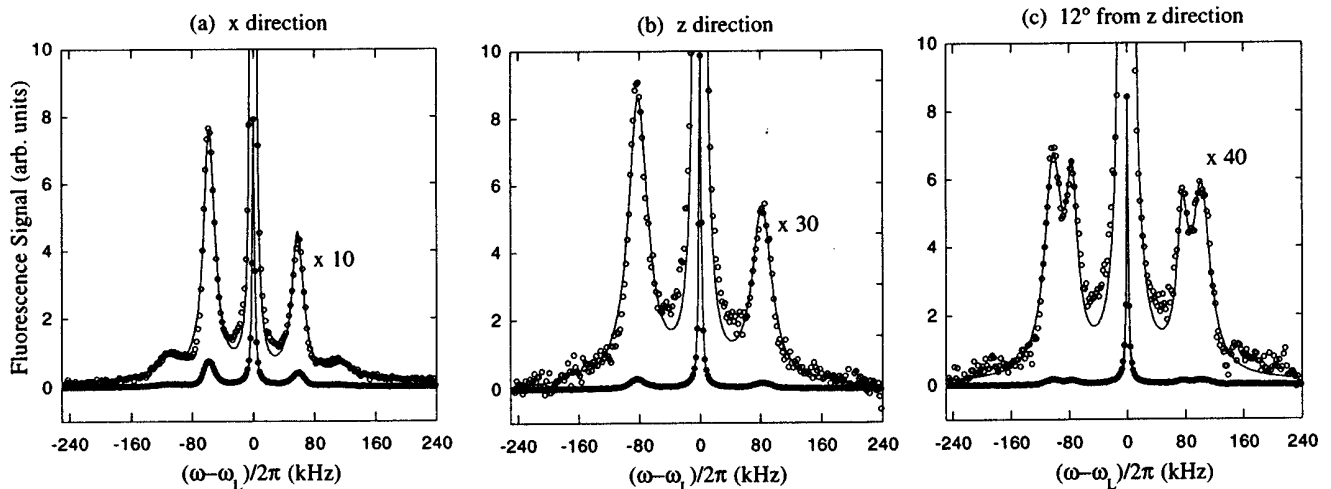


FIG. 2. Fluorescence spectra relative to the optical lattice laser frequency  $\omega_L$  taken with the same detuning and intensity along directions perpendicular (a) and parallel (b) to the symmetry axis  $z$  and along a direction making an angle of  $12^\circ$  with the  $z$  axis (c). The points are the data and the solid lines are five-Lorentzian fits: at  $\omega = \omega_L$ ,  $\omega_L \pm \Omega_{x,z}$ ,  $\omega_L \pm 2\Omega_{x,z}$  in (a), (b), respectively. In (c) the sidebands are at  $\omega_L \pm \Omega_x$  and  $\omega_L \pm \Omega_z$ .

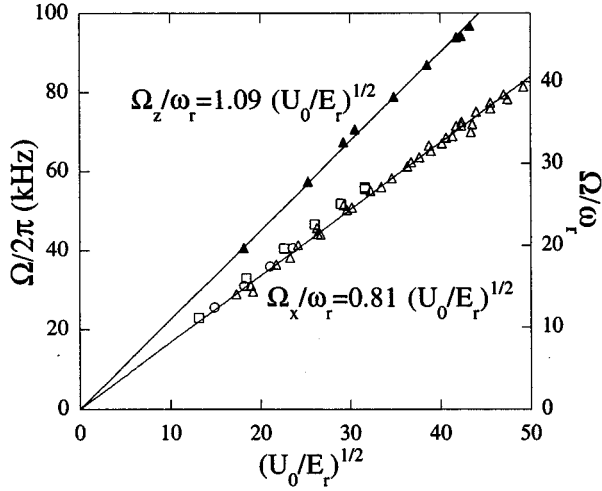


FIG. 3. Oscillation frequencies measured along directions parallel (solid) and perpendicular (open) to  $z$ , vs the square root of the scaled potential well depth  $(U_0/E_r)^{1/2}$ , at detunings of  $-5\Gamma$  ( $\blacktriangle$ ),  $-10\Gamma$  ( $\square$ ), and  $-15\Gamma$  ( $\circ$ ). The best fits to the data ( $\text{---}$ ) yield the slopes shown.

The spectra in Fig. 2 clearly exhibit the characteristics of scattering in the Lamb-Dicke regime: a narrow central peak from elastic scattering (instrumentally broadened) and inelastic side bands that indicate the oscillation frequency for motion in the wells of the lattice. We have observed the central peak with a higher resolution spectrum analyzer and found a Lorentzian shape with a full width at half maximum (FWHM) of 2.5 kHz, which we attribute partly to fluctuating phase shifts between the lattice beams and the local oscillator as a result of acoustic vibration of the optics. The existence of well resolved sidebands is an indication that the coherence time of the oscillatory motion of the atoms is longer than an oscillation period, which is much longer than the mean time between spontaneous scattering events. This surprising result, established by previous studies of optical lattices [1, 8–13], arises from the increased likelihood that the coherence of the motion is preserved following an absorption-spontaneous-emission cycle because of the tight binding of atoms to a harmonic potential [21]. The pronounced asymmetry of the intensity between the lower and upper sidebands results from the distribution of population among the different bound states of the wells [1].

In a harmonic approximation there is a single frequency for oscillatory motion along each principle axis  $\xi$ ,  $\Omega_\xi^{(0)}/\omega_r = (2K_\xi^2 U_0/m)^{1/2}/\omega_r = (2K_\xi/k)\sqrt{U_0/E_r}$ , where  $E_r = \hbar\omega_r = \hbar^2 k^2/2m$  is the recoil energy ( $\omega_r/2\pi = 2.07$  kHz for Cs). The wells in the 3D lattice are anisotropic ( $K_{x,y} = k/2$  and  $K_z = k/\sqrt{88/45}$ ), so there are two distinct frequencies:  $\Omega_{x,y}^{(0)}/\omega_r = \sqrt{U_0/E_r}$ ,  $\Omega_z^{(0)}/\omega_r = \sqrt{88U_0/45E_r}$  [22]. This is illustrated by the spectra shown in Figs. 2(a) and 2(b), which were measured along  $x$  and  $z$ , respectively. In addition, by observing the spectrum along a direction making a  $12^\circ$  angle with  $z$  in the  $x$ - $z$  plane we see both sideband frequencies simultaneously, as shown in Fig. 2(c) [23]. Figure 3 shows the dependence of the observed  $\Omega_x$  and  $\Omega_z$  on  $\sqrt{U_0}$ . The data clearly exhibit the  $\approx\sqrt{2}$  ratio between  $\Omega_x$  and  $\Omega_z$  and the expected scaling, independent of detuning, but fall 20% below the predictions of the harmonic model. This discrepancy,

well beyond our estimated 5% measurement uncertainty, is a consequence of anharmonicity of the potential [24], which we can treat perturbatively as a function of the parameter  $C = k_B T/2U_0$ . We find for a thermal distribution,  $\Omega_{x,y,z}(C) = \Omega_{x,y,z}^{(0)}(1 - 2C + \dots)$  along  $x$ ,  $y$ , and  $z$ , where  $\Omega_\xi^{(0)}$  is the harmonic frequency for the  $\xi$  direction. Given our measured value of  $C = 0.12$ , this analysis predicts frequencies in agreement with our measurements. In the 1D measurements of  $\Omega$ , from this experiment and from [1], there is a similar 20% discrepancy with the harmonic frequency,  $\Omega^{(0)}/\omega_r(88/45)\sqrt{U_0/E_r}$ . However, only about half of the discrepancy can be accounted for by anharmonicity. This may reflect the fact that the 1D experiment is not well within the classical regime [22] where our approximations are valid. In fact, a quantum Monte Carlo calculation of the 1D spectrum [2] is in good agreement with the results from [1].

The sidebands in our spectra are well fit by Lorentzians with line widths  $\Delta\Omega$  from 11 to 22 kHz (FWHM), which vary linearly with  $\sqrt{U_0}$  (and thus with  $\Omega$ ) and have a small positive intercept. This intercept width is approximately equal to the mean observed width of the central peak,  $\Delta\Omega_0/2\pi = 4.4(1.2)$  kHz (FWHM), which includes about 2 kHz of measured instrumental broadening. The linear scaling,  $(\Delta\Omega - \Delta\Omega_0)/\Omega = 0.26(4)$ , independent (within uncertainty) of both the detuning and observation direction in the 3D lattice, is consistent with broadening due to anharmonicity. From our perturbative treatment of anharmonicity we estimate  $\Delta\Omega/\Omega = 1.22C$  along  $z$  and  $1.53C$  along  $x$  in 3D. Since  $C = 0.12$ , this clearly accounts for much of the observed width. We also expect homogeneous broadening due to the decay of coherent oscillatory motion from inelastic scattering [21]. In the Lamb-Dicke regime an atom with vibration quantum number  $n$  inelastically scatters light at a rate  $\Gamma_n''$  that is smaller than the total spontaneous scattering rate,  $\Gamma' = \Gamma(U_0/\hbar\Delta)$ , by the localization factor,  $(k\xi_n)^2 \approx (2n+1)(k\xi_0)^2$ . Here,  $\xi_n$  is the spatial extent of the  $n$ th oscillator state. One might think that coherence between different oscillator states would decay at a similar rate giving the sidebands a width  $\approx\Gamma'$ . Our measured sidebands are much narrower, which is strong evidence for the transfer of coherence that is predicted to reduce this relaxation in the harmonic oscillator [25]. Anharmonicity limits the coherence transfer process so that relaxation due to inelastic photon scattering should contribute at the level of the anharmonicity width, but we have not calculated how these effects combine [26]. We note that, as in [1], the sideband width is nearly 30 kHz in the 1D lattice and is dominated by residual Doppler broadening.

In Figs. 2(a) and 2(b) the strength of the sidebands is markedly different for the spectra taken along the  $x$  and  $z$  directions. From the ratios  $\mathfrak{R}$  of the power in both first-order sidebands to that in the central peak, we determine localizations of  $x_{\text{rms}} = \lambda/7.3(0.7)$  and  $z_{\text{rms}} = \lambda/12(2)$  along  $x$  and  $z$ , respectively, in 3D, and  $x_{\text{rms}} = \lambda/18(2)$  in 1D, independent of laser intensity and detuning. (We note that our 1D result in Cs nearly agrees with the previous results in Rb [1]). When scaled to the curvature of the potential, our results are as follows:  $(kx_{\text{rms}})^2 = 0.122(16)$  in 1D and  $(K_x x_{\text{rms}})^2 = 0.183(18)$  and  $(K_z z_{\text{rms}})^2 = 0.143(25)$  in 3D, and can be used to infer the temperature coefficient  $C$  along each direc-

tion of observation. (Recall that  $\langle (K_\xi \xi)^2 \rangle = C$  in the harmonic approximation.) A proper determination of  $C$  in this way requires anharmonic corrections to the spatial distribution of atoms, as well as corrections to the vibrational motion and the resulting phase modulation which produces our spectrum. A correction for the first effect, by evaluating the second moment integral ( $\xi_{\text{rms}}^2 = \int d\mathbf{r}^3 \xi^2 \exp[-U(\mathbf{r})/k_B T]$ ) numerically using the full expression for the potential [10] yields a common value,  $C \approx 0.1$ . Although this is in good agreement with our TOF results, we expect the second correction to be of similar order.

Finally, as in [1] the sideband asymmetry evident in Fig. 2 may also be used to infer the temperature, which in 1D agrees within uncertainty with the TOF measurements, as shown in Fig. 1. In our 3D lattice the sample density is higher, and a density-dependent distortion of the spectrum occurs as a result of stimulated rescattering of fluorescence, as observed in probe propagation experiments [10–12]. We

have confirmed this by recording spectra at lower density and extrapolating to zero density, where the temperatures we infer are in good agreement with the TOF results.

We have measured the temperature of laser-cooled atoms in the well-defined field of an optical lattice in 3D and 1D by time of flight and from analysis of the fluorescence spectrum. The results imply a nearly common laser-cooling temperature  $kT/2 \approx 0.1 U_0$  and are in good agreement with a previous 1D experiment and with 1D quantum calculations. We hope these results will motivate a calculation of laser cooling in 3D, which is necessary for a quantitative comparison with experiment.

This work was supported in part by the U. S. Office of Naval Research, and in part by NSF Grant No. PHY-9312572. A. K. thanks the Swedish Natural Science Research Council (NFR) and G. B. thanks the Alexander von Humboldt Foundation for support. P. J. is supported by NSF Grant No. PHY-9503259.

- 
- [1] P. S. Jessen *et al.*, Phys. Rev. Lett. **69**, 49 (1992); P. S. Jessen, Ph.D. thesis, University of Aarhus, 1993 (unpublished).
- [2] P. Marte *et al.*, Phys. Rev. Lett. **71**, 1335 (1993).
- [3] Y. Castin and J. Dalibard, Europhys. Lett. **14**, 761 (1991).
- [4] Y. Castin and K. Molmer, Phys. Rev. Lett. **74**, 3772 (1995).
- [5] A. Steane and C. Foot, Europhys. Lett. **14**, 231 (1991); M. Drewsen *et al.*, Appl. Phys. **59**, 283 (1994).
- [6] C. Salomon *et al.*, Europhys. Lett. **12**, 683 (1990).
- [7] C. Gerz *et al.*, Europhys. Lett. **21**, 661 (1993).
- [8] P. Verkerk *et al.*, Phys. Rev. Lett. **68**, 3861 (1992).
- [9] A. Hemmerich and T. W. Hänsch, Phys. Rev. Lett. **70**, 410 (1993); Phys. Rev. A **48**, R1753 (1993).
- [10] G. Grynberg *et al.*, Phys. Rev. Lett. **70**, 2249 (1993); K. I. Petsas *et al.*, Phys. Rev. A **50**, 5173 (1994).
- [11] P. Verkerk *et al.*, Europhys. Lett. **26**, 171 (1994).
- [12] A. Hemmerich, C. Zimmermann, and T. W. Hänsch, Phys. Rev. Lett. **72**, 625 (1994).
- [13] A. Hemmerich, M. Weidemüller, and T. Hänsch, Europhys. Lett. **27**, 427 (1994).
- [14] A. Kastberg *et al.*, Phys. Rev. Lett. **74**, 1542 (1995).
- [15] Using  $n+1$  beams in  $n$  dimensions ensures that the morphology of the optical potential does not depend on the  $n$  relative phase differences between the beams (see [10]). The entire pattern simply translates in space as these phases vary in time. In our experiments, we expect the evolution of the beam phases to occur on a time scale slow enough that the atoms can adiabatically follow the lattice translations, so we ignore them.
- [16] In accordance with the standard convention, we will use the diabatic potentials of the most light shifted ground states ( $F=4$ ,  $m_F=\pm 4$ ) to describe the optical lattice. The factor (44/45) comes from Clebsch-Gordan coefficients for  $F=4$  to  $F'=5$ .
- [17] R. Dicke, Phys. Rev. **89**, 472 (1953).
- [18] D. J. Wineland and Wayne M. Itano, Phys. Rev. A **20**, 1521 (1979). We define  $\mathfrak{R}$  as the ratio of the power in both first-order sidebands to the carrier. From their equation (44), for  $k_B T \gg \hbar \Omega_\xi$  and  $k^2 \langle \xi^2 \rangle \ll 1$ ,
- $$\mathfrak{R} = (k \xi_{\text{rms}})^2 - (k \xi_{\text{rms}})^6/8 + \dots$$
- [19] C. I. Westbrook *et al.*, Phys. Rev. Lett. **65**, 33 (1990).
- [20] C. Jurczak *et al.*, Phys. Rev. Lett. **77**, 1727 (1996).
- [21] J.-Y. Courtois and G. Grynberg, Phys. Rev. A **46**, 7060 (1992).
- [22] This result obtains only in the high temperature classical limit ( $kT/\hbar\Omega \approx 2C(k/2K)(U_0/\omega_r)^{1/2} \gg 1$ ). In this experiment,  $3 \leq kT/\hbar\Omega \leq 8$  in 3D along  $x$  and  $1.4 \leq kT/\hbar\Omega \leq 4$  in 1D.
- [23] At this angle we expect to see four times as much integrated intensity in the  $z$ -direction sidebands as in the  $x$ -direction sidebands. In contrast, the spectrum shown in Fig. 2(c) has only twice the intensity in  $z$  as in  $x$ .
- [24] We use the diabatic expression for the potential because its analytic form allows a simple model to be developed, and the difference between the diabatic potential and the harmonic approximation is substantially larger than the difference between the diabatic and adiabatic potentials.
- [25] C. Cohen-Tannoudji, J. Dupont-Roc, and G. Grynberg, *Atom-Photon Interactions* (Wiley, New York, 1992), p. 328.
- [26] The calculations of the decay rate in [21] applies only to a harmonic potential, where the decay of  $(n, n+1)$  coherences feed  $(n-1, n)$  coherences, just as  $n+1$  population feeds  $n$  population, causing a *net* coherence decay that resembles energy decay. When anharmonicity begins to become important the coherence decay rate increases due to the loss of this coherence transfer between levels which no longer have the same energy difference. This effect is difficult to model.